

Characteristics of the Greenhouse Gas Concentration Derived from the Ground-based FTS Spectra at Anmyeondo, Korea

5 Young-Suk Oh^{1,2*}, Samuel Takele Kenea¹, Tae-Young Goo¹, Kyu-Sun Chung², David W. T. Griffith³, Paul. Wennberg⁴, Voltaire A. Velazco³, Jae-Sang Rhee¹, Mi-Lim Ou⁵, and Young-Hwa Byun¹

1. Climate Research Division, National Institute of Meteorological Sciences (NIMS), Jeju-do, Republic of Korea
2. Department of Electrical Eng. & Centre for Edge Plasma Science, Hanyang University, Seoul, Republic of Korea
- 10 3. School of Chemistry, University of Wollongong, Wollongong, Australia
4. California Institute of Technology, California, USA
5. Climate Change Monitoring Division, Korea Meteorological Administration, Seoul, Republic of Korea

*Correspondence to: Young-Suk Oh (ysoh306@gmail.com)

15 Abstract.

Since the late 1990s, the meteorological observatory established in Anmyeondo (36.5382° N, 126.3311° E, and 30 m above mean sea level), has been monitoring several greenhouse gases such as CO₂, CH₄, N₂O, CFCs, and SF₆, as part of the Global Atmosphere Watch (GAW) Program. A high resolution ground-based (g-b) Fourier Transform Spectrometer (FTS, IFS-125HR model) was installed at such observation site in 2013, and has been fully operated within the frame work of the Total Carbon Column Observing Network (TCCON) since August, 2014. The solar spectra recorded by the g-b FTS are covered in the range between 3,800 and 16,000 cm⁻¹ at the spectral resolution of 0.02 cm⁻¹ during the measurement period between 2014 and 2016. In this work, the GGG2014 version of the TCCON standard retrieval algorithm was used to retrieve XCO₂ concentrations from the FTS spectra. Two spectral bands (at 6220.0 and 6339.5 cm⁻¹ centre wavenumbers) were used to derive the XCO₂ concentration within the spectral residual of +0.01 %. All sources of errors were thoroughly analyzed. In this paper, we introduced aircraft observation campaigns over Anmyeondo station were carried out during the period between 2012 and 2016. A comparison of the XCO₂ concentration in g-b FTS and OCO-2 (Orbiting Carbon Observatory) satellite observations was presented only for the measurement period between February 2014 and December 2016. The 13 coincident observations were selected on a daily median basis. It was obtained that OCO-2 exhibited slightly higher bias with respect to the g-b FTS, which is about 0.189 ppm with the standard deviation of 1.19 ppm, and revealed a strong correlation (R=0.94). Based on seasonal cycle comparisons, both instruments generally agreed in capturing seasonal variations of the target species with its maximum and minimum values in spring and late summer, respectively. In the future, it is planned to exert further works in utilizing the FTS measurements for the evaluation of satellite observations such as Greenhouse Gases Observing Satellite (GOSAT) at observation sites. This is the first report of the g-b FTS observations of XCO₂ species over the Anmyeondo station.

40 **Key words:** Aircraft, XCO₂, OCO-2, TCCON, Infrared spectra

1. Introduction

Monitoring of greenhouse gases (GHGs) is a crucial issue in the context of the global climate change. Carbon dioxide (CO₂) is one of the key greenhouse gas and its global annual mean concentration has been increased rapidly from 278 to 400 ppm since 1750, pre-industrial year (WMO greenhouse gas
45 bulletin, 2016). Radiative forcing of atmospheric CO₂ accounts for approximately 65 % of the total radiative forcing by long-lived GHGs (Ohyama et al., 2015 and reference therein). Human activities, such as burning of fossil fuels, land use change, etc., are the primary drivers of the continuing increase in atmospheric greenhouse gases and the gases involved in their chemical production (Kiel et al., 2016 and reference therein). In the fact that it is a global concern for demanding accurate and precise long-
50 term measurements of greenhouse gases.

In the field of remote sensing techniques, solar absorption infrared spectroscopy is an essential technique, which has been increasingly used to determine changes in atmospheric constituents. Nowadays, a number of instruments deployed in various platforms (e.g., ground-based, space-borne) have been operated for measuring GHGs such as CO₂. Our g-b FTS at the Anmyeondo station has been
55 measuring several atmospheric GHGs such as CO₂, CH₄, CO, N₂O, and H₂O operated within the framework of the Total Carbon Column Observing Network (TCCON). XCO₂ retrievals from the g-b FTS have been reported at different TCCON sites (e.g, Ohyama et al., 2009; Deutscher et al., 2010; Messerschmidt et al., 2010, 2012; Miao et al., 2013; Kivi and Heikkinen, 2016). TCCON achieves the accuracy and precision in measuring the column averaged dry air mole fraction of CO₂ (XCO₂), as
60 about 0.25 % that is less than 1 ppm (Wunch et al., 2010), which is essential to get information about sinks and sources, as well as validating satellite products (Rayner and O'Brien, 2001; Miller et al., 2007). It is reported that the precision of CO₂ even 0.1 % can be achieved during clear sky conditions (Messerschmidt et al., 2010; Deutscher et al., 2010). The network aims to improve global carbon cycle studies and supply the primary validation data of different atmospheric trace gases derived from space-
65 based instruments, e.g., the Orbiting Carbon Observatory 2 (OCO-2), the Greenhouse Gases Observing Satellite (GOSAT) (Morino et al., 2011; Frankenberg et al., 2015).

The objective of this study is focused on the characteristics of XCO₂ concentration retrievals from g-b FTS spectra and is implement a preliminary comparison against OCO-2 over the Anmyeondo station. The FTS spectra have been processed using the TCCON standard GGG2014 (Wunch et al., 2015)
70 retrieval software. One of the interesting issues in this work is a new home made addition to our g-b FTS instrument that reduces the solar intensity variations from the 5% maximum allowed in TCCON to less than 2%. This paper presents introduction to instrumentation and measurement site, and next to that, provides results and discussion followed by conclusions.

2.1 Station description

The G-b FTS observatory was established in the Anmyeondo (AMY) station, which is located at 36.32° N, 126.19° E, and 30 m above sea level. This station is situated on the west coast of the Korean Peninsula, which is 180 kilometres away from Seoul, the capital city of Republic of Korea. Figure 1 displays the Anmyeondo station. It is also a regional GAW (Global Atmosphere Watch) station that belongs to the Climate Change Monitoring Network of KMA (Korean Meteorological Administration). The AMY station has been monitoring various atmospheric compositions such as greenhouse gases, aerosols, ultraviolet radiation, ozone, and precipitation since 1999. The total area of Anmyeondo is estimated to be ~87.96 km² and approximately 1.25 million people reside in this island. Some of the residents over this area are engaged in agricultural activities. Vegetated areas consisting of mainly pine trees are located in and around the FTS observatory. The topographic feature of the area consists of low level hills, on average it is about 100 m above sea level. The climatic condition of the area is: the minimum temperature occurred on winter season with an average of 2.7 °C, and the maximum temperature is about 25.6 °C during summer season. In addition, the annual precipitation amount is estimated to be 1,155 mm; and the high amount of snows would be observed in winter. Such a observation site has been designated as part of TCCON site since August 2014. The AMY Station's on TCCON wiki page is kept available and can be found at: [<https://tcon-wiki.Anmyeondo.edu>]

2.2 G-b FTS instrument

Solar spectra are acquired by operating a Bruker IFS 125HR spectrometer (Bruker Optics, Germany) under the framework of TCCON. Currently, our g-b FTS instrument operation is semi-automated for taking the routine measurements under clear sky conditions. It is planned to make an FTS operation mode to be fully automated by this year. The solar tracker (Tracker A547, Bruker Optics, Germany) is mounted inside a dome. The tracking ranges in terms of both azimuthal and elevation angles are about 0 to 315 and -10 to 85 degrees, respectively, while the tracking speed is about 2 degrees per second. The tracking accuracy of ±4 minutes of arc can be achieved by the Camtracker mode. Under clear sky conditions, the dome is opened and set to an automatic-turning mode, in order that the mirrors are moved automatically to search for the position where the sunspot is seen by the camera. Then, the solar tracker is activated in such a way that the mirrors are finely and continuously controlled to fix the beam into the spectrometer. Figure 2 displays an overview of the general data acquisition system. This ensures that all spectra were recorded under clear weather conditions. The other important feature that has been made on the FTS spectrometer is the implementation of the interferogram sampling method (Brault, 1996), that takes advantage of modern analogue-digital converters (ADCs) to improve the signal-to-noise ratio.

The spectrometer is equipped with two room temperature detectors; an Indium-Gallium-Arsenide (InGaAs) detector, which covers the spectral region from 3,800 to 12,800 cm^{-1} , and Silicon (Si) diode detector (9,000 – 25,000 cm^{-1}) used in a dual-acquisition mode with a dichroic optic (Omega Optical, 10,000 cm^{-1} cut-on). A filter (Oriel Instruments 59523; 15,500 cm^{-1} cut-on) prior to the Si diode detector blocks visible light, which would otherwise be aliased into a near-infrared spectral domain. TCCON measurements are routinely recorded at a maximum optical path difference (OPD_{max}) of 45 cm leading to a spectral resolution of 0.02 cm^{-1} . Two scans, one forward and one backward, are performed and individual interferograms are recorded. As an example, Figure 3 shows a single spectrum recorded on 4 October 2014 with a resolution of 0.02 cm^{-1} . A single scan in one measurement takes about 110 s. Measurement setting for the Anmyeondo g-b FTS spectrometer of the Bruker 125HR model is summarized in Table 1. The pressure inside FTS is kept at 0.1 to 0.2 hPa with vacuum pump to maintain the stability of the system and to ensure clean and dry conditions.

2.3 Characterization of FTS-instrumental line shapes

For the accurate retrieval of total column values of the species of interest, a good alignment of the g-b FTS is essential. The instrument line shape (ILS) is retrieved from the regular HCl cell measurement that is an important indicator of the status of the FTS's alignment (Hase et al., 1999). The analyses of the measurements were performed using a linefit spectrum fitting algorithm (LINEFIT14 software) (Hase et al., 2013). Here, we have carried out experiments to investigate the influences of ILS. We showed the time series of the phase error (rad) (left panel) and modulation efficiency (right panel) in the HCl measurement using the source of light from tungsten lamp in the period of October 2013 to September 2017, which is depicted in Figure 4. Modulation amplitudes for well alignment should be controlled in a limit of 5 % loss at the maximum optical difference (Wunch et al., 2011). In our g-b FTS measurements, it is found that the maximum loss of modulation efficiency is less than 1 %, which is quite close to the ideal value. The phase errors are less than 0.0001. Hase et al. (2013) reported that this level of small disturbances from the ideal value of the modulation efficiency is common to all well-aligned instruments. This result confirmed that the g-b FTS instrument is well aligned and stable during the whole operation period.

We also confirmed that the ILS was not affected by the variable aperture during the operation of this system. The modulation efficiency and phase error were estimated to be 99.98 % and 0.0001 rad. Sun et al. (2017) reported the detailed characteristics of the ILS with respect to applications of different optical attenuators to FTIR spectrometers within the TCCON and NDACC networks. They used both lamp and sun cell measurements which were conducted after the insertion of five different attenuators in front of and behind the interferometer. In Sun et al. (2017), the ILS result was indicated by considering optical attenuator number 1 which is in good agreement with our findings.

2.4 Data processing

145 Within the TCCON standard retrieval strategy, we have derived the column-averaged dry-air mole fraction CO₂ (XCO₂) and other atmospheric gases (O₂, CO, CH₄, N₂O, and H₂O) using GFIT algorithm. The spectral windows used for the retrieval of CO₂ and O₂ are given in Table 2. The TCCON standard GGG2014 (version 4.8.6) retrieval software was used to obtain the abundance of the species from FTS spectra (Wunch et al., 2015). The XCO₂ is the ratio of retrieved CO₂ column to retrieved O₂ column,

$$150 \quad XCO_2 = \frac{CO_2 \text{ column}}{O_2 \text{ column}} \times 0.2095, \quad (1)$$

Computing the ratio using Eq. (1) minimizes systematic and correlated errors such as errors in solar zenith angle, surface pressure, and instrumental line shape that existed in the retrieved CO₂ and O₂ columns (Washenfelder et al., 2006, Messerschmidt et al., 2012). Top panel of Fig.6 depicts the time series of laser sampling error (LSE) obtained from InGaAs spectra at the Anmyeondo FTS station in the measurement period of February 2014 to December 2016. LSE is small and centered around zero in an ideal case. Slightly large LSE values were shown on 10 March, 2014 (see top panel of Fig. 7). On this date, we conducted the laser adjustment in FTS.

The X_{air} is a useful indicator of the quality of measurements and the instrument performance. The X_{air} would be unity for an ideal retrieval, however, due to spectroscopic limitations there is a TCCON wide bias and solar zenith angle (SZA) dependence. The retrieval of X_{air} deviating more than 1% from the nominal value of 0.98 would suggest a systematic error. The time series of X_{air} is shown in the bottom panel of Figure 5. The X_{air} record reveals that the instrument has been stable during the measurement period. It shows that the values of X_{air} are fluctuated between 0.974 and 0.985, and the mean value is 165 0.982 with a standard deviation of 0.0015 in which the scatter for X_{air} is about 0.15 %. The low variability in time series of X_{air} indicates the stability of the measurements.

2.5 Aircraft observation campaigns over Anmyeondo station

In this section, we have discussed a preliminary comparison results made between aircraft observations and g-b FTS over the Anmyeondo station. The aircraft campaign conducted over Anmyeondo station was monitored by National Institute of Meteorological Sciences (NIMS). The aircraft was equipped with a Wavelength Scanned Cavity Ring Down Spectrometer (CRDS; Picarro, G2401-mc) providing mixing ratio data recorded at 0.3 Hz intervals. The position of the aircraft was monitored by GPS, and information on the outside temperature, static pressure, and ground speed was provided by the aircraft's instruments. Data observed during ascent and descent of the aircraft are considered as vertical profiles of CO₂ and CH₄ over the measurement station. The temperature and pressure of the gas sample have to be tightly controlled at 45 °C and 140 Torr in the CRDS, which leads to highly stable spectroscopic features (Chen et al., 2010). Any deviations from these values cause a reduction of the instrument's

precision. Data recorded beyond these range of variations in cavity pressure and temperature were discarded in this analysis. Variance of the cavity pressure and temperature in flight result in variance in the CO₂ and CH₄ mixing ratios. The Picarro CRDS instrument has been regularly calibrated with respect to the standard gases within the error range recommend by World Meteorological Organization (CO₂ is 380.23 ± 0.1 ppm, CH₄ is 1.825 ± 0.001 ppm)

Several aircraft observation campaigns over Anmyeondo station were carried out during the period between 2012 and 2016. However, a few numbers of aircraft data matched with the remote sensing instruments were available during this observation period. The total number of the aircraft measurements that matched with g-b FTS was only three and all those coincident observations were laid within a period of 2015. The g-b FTS retrieval of XCO₂ and XCH₄ were compared with aircraft measurements. Here, FTS data were averaged over a time window of ± 30 minutes with respect to the aircraft measurement time. In addition, the averaging kernel of the FTS was applied into the aircraft data. The g-b FTS data were corrected for an airmass-dependent artefact for XCO₂ and XCH₄, as well as calibrated with respect to TCCON common scaling factors. This scale factor was derived empirically using aircraft profiles over many TCCON sites in order to place the TCCON data on the WMO standard reference scales (Wunch et al. 2010) for both XCO₂ and XCH₄. This comparison study will be useful for ensuring that the TCCON common scale factors can be applied to our g-b FTS data. The statistical results for XCO₂ and XCH₄ comparisons between aircraft and g-b FTS are summarized in Table 3. The mean absolute difference between FTS and aircraft were found to be -0.798 ± 1.734 ppm, the corresponding mean relative differences of -0.196 ± 0.427 % for XCO₂, while the mean absolute difference of XCH₄ is -0.0079 ± 0.012 ppm, with a corresponding mean relative difference of -0.426 ± 0.632 %. These differences appeared on both species were consistent with the combined total errors of instruments. Wunch et al. (2010) reported that the uncertainties (2σ) of the TCCON common scale are approximately 0.2 % for XCO₂ and 0.4 % for XCH₄. It is determined that our g-b FTS uncertainty was found to be within this range of uncertainties and can be calibrated against WMO standard scale. Here, we also include some results from the aircraft campaign conducted in 2016, which was operated by KORUS-AQ (Korea-U.S.-Air Quality) joint program aiming at advancing the ability to monitor air pollution from space. Figure 6 illustrates the results of XCO₂ and XCH₄ comparisons between the aircraft observation and TCCON sites data. Light blue diamond marks show for Anmyeondo station. Our results laid within the indicated linear regression curves as with other TCCON sites.

2.6 OCO-2

Orbiting Carbon Observatory-2 (OCO-2) is NASA's first Earth-orbiting satellite, which was successfully launched on July 2, 2014 into low-Earth orbit. It is devoted to observing atmospheric

carbon dioxide (CO₂) to get better insight for the carbon cycle. The primary mission is to measure carbon dioxide with high precision and accuracy in order to characterize its sources and sinks at different spatial and temporal scales (Boland et al., 2009; Crisp, 2008, 2015). The instrument measures the near infrared spectra (NIR) of sunlight reflected off the Earth's surface. Using a retrieval algorithm, it provides results of atmospheric abundances of carbon dioxide and related atmospheric parameters at the nadir, sun glint and targets modes. Detailed information about the instrument is available in different papers (Connor et al., 2008; O'Dell et al., 2012). In this work, we used the OCO-2 version 7Br bias corrected data.

220 **3 Results and discussion**

3.1 Time series of g-b FTS XCO₂, seasonal and annual cycle

The time series of XCO₂ along with retrievals of other trace gases such as XCO and XCH₄ from g-b FTS is presented in Figure 7 (panel a-c) during the period from February 2014 to December 2016. In such time series plots, each marker represents single retrievals, and the fitting curves of the retrieved values are also depicted (red solid line). We showed the seasonal cycle of XCO₂, XCO, and XCH₄ in the time series using a fitting procedure described by Thoning et al. (1989). Standard deviations of the differences between the retrieved values and the fitting curves are 1.42 ppm, 11.0 ppb, and 10.3 ppb for XCO₂, XCO, and XCH₄, respectively. It is evident that all species have a feature of seasonal cycle. Year to year variability of XCO₂ is highest in spring and lowest during the growing season in June to September. Moreover, the behavior of seasonal cycle of XCO₂ at our site was compared with that of XCO₂ at Saga, Japan, which is discussed in later section. The atmospheric increase of XCO₂ from 2015 to 2016 was 3.65 ppm which is larger than the increase from 2014 to 2015. For the case of XCH₄, its increase from 2015 to 2016 was 0.02 ppm which is higher than the increase from 2014 to 2015, whereas in XCO the rate of increment from year to year was found to be slightly decreased (see Table 4).

235 Moreover, the seasonal and annual cycles of XCO₂ derived from the g-b FTS were compared with in-situ tower observations of CO₂ over the Anmyeondo station, which are presented in Figure 8. Regarding in-situ data, samples were collected using flask using non-dispersive infrared (NDIR) method at the altitude of 77 meters above sea level at Anmyeondo station (36.53 N, 126.32 E) (details about data are available at <http://ds.data.jma.go.jp/jmd/wdcgg/>). Nearly 97 % of in-situ data were taken during day time between 04:00 – 08:40 UTC (13:00 – 17:40 Korea Standard Time (KST)) so that the early morning and night time observations of CO₂ were almost neglected. In-situ CO₂ monthly means are generated by first averaging all valid event measurements with a unique sample date and time. The values are then extracted at weekly intervals from a smooth curve (Thoning et al., 1989) fitted to the averaged data and then these weekly values are averaged for each month. As can be seen in Figure 8, the overall patterns of seasonal and annual cycle of FTS XCO₂ tend to be similar with that of in-situ tower CO₂ over there.

This could suggest that the amplitude of seasonal cycle was likely to be driven by the imbalance of ecosystem exchange.

3.2 Correlations between XCO₂ and XCO

CO is co-emitted with CO₂ from combustion sources, leading to a significant positive correlation between them when combustion is a significant source of observed CO₂. The midday peaks for each gas reflect the influence of anthropogenic emissions. To examine this effect, we have determined the correlations between ΔXCO and ΔXCO_2 at our site. In order to compute the correlations, first we have selected hourly averaged data for both XCO and XCO₂ that were recorded between 06:00 and 07:00 UTC (i.e 15:00 and 16:00 LST, local standard time), excluding summer data, and then calculated the anomalies by subtracting the hourly averaged data from the mean of the selected data during the measurement period of February 2014 to December 2016. Figure 9 depicts the relationship between hourly CO₂ and CO means of anomalies at Anmyeondo during the whole measurement period, excluding summer data. CO₂ and CO had a correlation of 0.50, and this suggests that there is an influence of combustion emissions on CO₂. However, in a summer season, a negative relationship between them was identified at this site, with the small magnitude of correlation -0.22, and a correlation slope of -0.84. In Ohyama et al., (2015) paper, they derived the correlation coefficients and slopes of $\Delta XCO/\Delta XCO_2$ and $\Delta XCH_4/\Delta XCO$ in order to understand the short term variations of XCO₂, XCO, and XCH₄ in summer seasons during July 2011 and December 2014 at Saga, Japan. The trajectories for the summer season were classified into three types, depending on the origin of the air masses. The trajectories for types I, II, and III relate to transport of air masses from the Asian continent (China), Southeast Asia, and the Pacific Ocean, respectively. The negative slope of the $\Delta XCO/\Delta XCO_2$ ratio for the type I (slope was -3.15 ppb ppm⁻¹) gentler than for the type II (slope was -14.3 ppb ppm⁻¹), which was due to the transport of the air masses that experience the strong biospheric uptake of CO₂ over the Asia. This argument could support for our analysis at Anmyeondo station. The slope that we obtained in our station is close to the slope reported in type III case in Ohyama et al., (2015) paper.

In Wang et al (2010), the diurnal cycles of CO₂ signal was dominated by the biospheric activity from May to September, with a maximum drawdown of 39 ppmv in daily CO₂ in the summer at rural station near Beijing. Biospheric activity, however, has little impact on CO except for the CO source from in situ oxidation of biogenic hydrocarbons. They obtained that the correlation between CO₂ and CO in summer was insignificant. The correlation slope gives the emission ratio of CO to CO₂, which fluctuates with the sources of CO₂, depending on different combustion types and biospheric activity. In our case, the correlation slope of CO to CO₂ was found to be 2.27 ppb ppm⁻¹ during the whole measurement period excluding summer, which is smaller than the correlation slope reported in Hefei FTS station where it was estimated to be 5.66 ppb ppm⁻¹ (Wang et al., 2017 and references therein), which are primarily attributed to the smaller emission in CO.

3.3 Comparison of Anmyeondo XCO₂ with nearby TCCON station

We presented the comparison of our FTS XCO₂ data with a similar ground-based high resolution FTS observation at Saga TCCON station (33.26 N, 130.29 E) in Japan, which is the closest TCCON station to our site. Among those TCCON station, Rikubetsu, Tsukuba, and Saga are located in Japan (Morino et al., 2011, Ohyama et al., 2009, 2015) and Hefei is located in China (Wang et al., 2017). To demonstrate the comparison between them, we have shown the daily averaged XCO₂ of two stations during the period of 2014 to 2016 in Figure 10. As can be seen, variations of XCO₂ at the Saga station agreed well with Anmyeondo station. The daily averaged XCO₂ revealed the same seasonal cycle as that of our station. The lowest XCO₂ appeared in late summer (August and September), and the highest value was in spring (April).

Ohyama et al., (2015) studied the time series of XCO₂ at Saga, Japan during the period from July 2011 to December 2014. They showed seasonal and interannual variations over there. The peak-to-peak seasonal amplitude of XCO₂ was 6.9 ppm over Saga during July 2011 and December 2014, with a seasonal maximum and minimum in the average seasonal cycle during May and September, respectively. In recent finding of Wang et al. (2017), the g-b FTS temporal distributions of XCO₂ at Hefei, China were reported. The FTS observations in 2014 to 2016 had a clear seasonal cycle XCO₂ reaches a minimum in late summer, and then slowly increases to the highest value in spring. The daily average of XCO₂ ranges from 392.33 ± 0.86 to 411.62 ± 0.90 ppm, and the monthly average value shows a seasonal amplitude of 8.31 and 13.56 ppm from 2014 to 2015 and from 2015 to 2016, respectively. The seasonal cycle was mainly driven by biosphere–atmosphere exchange. Butz et al., (2011) reported that the observations from GOSAT and the co-located ground-based measurements agreed well in capturing the seasonal cycle of XCO₂ with the late summer minimum and the spring maximum for four TCCON stations (Bialystok, Orleans, Park Falls, and Lamont) in the Northern Hemisphere. We inferred that the variation of XCO₂ over Anmyeondo station is in harmony with the variation pattern in elsewhere in mid-latitude Northern Hemisphere.

3.4 Comparison of XCO₂ between the g-b FTS and OCO-2

In this section, we present a comparison of XCO₂ between the g-b FTS and OCO-2 version 7Br data (bias corrected data) over Anmyeondo station during the period between 2014 and 2016. For making a direct comparison of the g-b FTS measurements against OCO-2, we applied the spatial coincidence criteria for the OCO-2 data within 3° latitude/longitude of the FTS station, as well as setting up a time window of 3 hours (maximum 3 h mismatch between satellite and g-b FTS observations). Based on the coincidence criteria, we obtained 13 coincident measurements, which were not sufficient to infer a robust conclusion. But it gives a preliminary result for indicating a level of agreement between them. The comparison of the time series of XCO₂ concentrations derived from the g-b FTS and OCO-2 on daily medians basis are demonstrated during the measurement period between 2014 and 2016, as

depicted in Figure 11. As can be seen in the plot, the g-b FTS measurement exhibits some gaps occurred due to bad weather conditions, instrument failures, and absences of an instrument operator. In the present analysis, the XCO₂ concentrations from FTS were considered only when its retrieval error was below 1.50 ppm (it is not shown here), which is the sum of all error components such as laser sampling error, zero level offsets, ILS error, smoothing error, atmospheric apriori temperature, atmospheric apriori pressure, surface pressure, and random noise. Wunch et al. (2016) reported that the comparison of XCO₂ derived from the OCO-2 version 7Br data against a co-located ground-based TCCON data that indicates the median differences between the OCO-2 and TCCON data were less than 0.50 ppm, a corresponding RMS differences less than 1.50 ppm. The overall results of our comparisons were comparable with the report Wunch et al. (2016). The OCO-2 product of XCO₂ was biased (satellite minus g-b FTS) with respect to the g-b FTS, which was slightly higher by 0.18 ppm with a standard deviation of 1.19 ppm, a corresponding RMS difference of 1.16 ppm. This bias could be attributed to the instrument uncertainty. In addition to that, we also obtained a strong correlation between them, which was quantified as a correlation coefficient of 0.94 (see Table 5).

Moreover, both instruments are generally agreed in capturing the seasonal variability of XCO₂ at the measurement station. As can be seen clearly from the temporal distribution of FTS XCO₂, the maximum and minimum values are discernible in spring and late summer seasons, respectively. It was found that its mean values in spring and summer were 402.72 and 396.92 ppm, respectively (see Table 6). This is because the seasonal variation of XCO₂ is most likely to be controlled by the imbalance of the terrestrial ecosystem exchange, and this could explain the larger XCO₂ values in the northern hemisphere in late April (Schneising et al. 2008, and references therein). The minimum value of XCO₂ occurs in August, which is most likely due to uptake of carbon into the biosphere in associated with the period of plant growth. Furthermore, both instruments showed high standard deviations during summer, which are about 3.28 ppm in FTS and 3.77 ppm in OCO-2, and this suggests that the variability reflects strong sources and sink signals.

4 Conclusions

Monitoring of greenhouse gases is an essential issue in the context of the global climate change. Accurate and precise continuous long-term measurements of the greenhouse gases (GHGs) are substantial for investigating their source and sinks. Nowadays, several remote sensing instruments operated on different platforms are dedicated for measuring GHGs. Greenhouse gases such as XCO₂, XCH₄, XH₂O, XN₂O measurements have been made using the g-b FTS at the Anmyeondo station since 2013. However, in this work, we focused on the measurements taken during the period of February 2014 to December 2016. The instrument has been operated in a semi-automated mode since then. The FTS instrument has been stable during the whole measurement period. Regular instrument alignments using the HCl cell measurements are performed. Thus, it guarantees the quality of the spectra. The

TCCON standard GGG2014 retrieval software was used to retrieve XCO₂, XCO, and others GHG gases from the g-b FTS spectra.

In this work, the g-b FTS retrieval of XCO₂ and XCH₄ were compared with aircraft measurements that were conducted over Anmyeondo station. We obtained the mean absolute difference between FTS and aircraft were found to be -0.798 ± 1.734 ppm, the corresponding mean relative differences of -0.196 ± 0.427 % for XCO₂, while the mean absolute difference of XCH₄ is -0.0079 ± 0.012 ppm, with a corresponding mean relative difference of -0.426 ± 0.632 %. These differences appeared on both species were consistent with the combined total errors of instruments. The preliminary comparison results of XCO₂ between FTS and OCO-2 were also presented over the Anmyeondo station. The mean absolute difference of XCO₂ between FTS and OCO-2 was calculated on daily median basis, and it was estimated to be 0.18 ppm with a standard deviation of 0.19 with respect to the g-b FTS. This bias could be attributed with instrument uncertainty. Based on the seasonal cycle comparison, both the g-b FTS and OCO-2 illustrated a consistent pattern in capturing the seasonal variability of XCO₂, with maximum in spring and minimum in summer. In summer and fall, plants flourish and CO₂ is most likely to be consumed by photosynthesis. However, in winter and spring, weak photosynthesis phenomenon would be expected to occur because of low plant flourishing and CO₂ reaches the highest values particularly in April. Therefore, the outcome of this study reflects the suitability of the measurements for improving the understanding of the carbon cycle, as well as evaluating the remote sensing data.

5 Acknowledgements

This research was supported by the Research and Development for KMA Weather, Climate, and Earth system Services (NIMS-2016-3100). We would greatly acknowledge the two anonymous reviewers who helped us to improve this manuscript well.

References

- Boland, S., Brown L. R., Burrows J. P., Ciais P., Connor B. J., Crisp D., Denning S., Doney S. C., Engelen R., Fung I. Y., Griffith P., Jacob D. J., Johnson B., Martin-Torres J., Michalak A. M., Miller C. E., Polonsky I., Potter C., Randerson J. T., Rayner P. J., Salawitch R. J., Santee M., Tans P. P., Wennberg P. O., Wunch D., Wofsy S. C., and Yung Y. L.: The Need for Atmospheric Carbon Dioxide Measurements from Space: Contributions from a Rapid Reflight of the Orbiting Carbon Observatory, 2009, http://www.nasa.gov/pdf/363474main_OCO_Reflight.pdf.
- Brault, J. W.: New approach to high-precision Fourier transform spectrometer design. Appl. Opt. 35, 2891–2896, 1996.
- Butz, A., Guerlet, S., Hasekamp, O., Schepers, D., Galli, A., Aben, I., Frankenberg, C., Hartmann, J.-M.,

- Tran, H., Kuze, A., Keppel-Aleks, G., Toon, G., Wunch, D., Wennberg, P., Deutscher, N., Griffith, D., Macatangay, R., Messerschmidt, J., Notholt, J., and Warneke, T.: Toward accurate CO₂ and CH₄ observations from GOSAT, *Geophys. Res. Lett.*, 38, L14812, <https://doi.org/10.1029/2011GL047888>, 2011.
- Chen, H., Winderlich, J., Gerbig, C., Hofer, A., Rella, C. W., Crosson, E. R., Van Pelt, A. D., Steinbach, J., Kolle, O., Beck, V., Daube, B. C., Gottlieb, E. W., Chow, V. Y., Santoni, G. W., and Wofsy, S. C.: High-accuracy continuous airborne measurement of greenhouse gases (CO₂ and CH₄) using the cavity ring-down spectroscopy (CRDS) technique *Atmos. Meas. Tech.*, 3, 375-386, 2010.
- Connor B. J., Bösch H., Toon G., Sen B., Miller C. E., and Crisp D.: Orbiting carbon observatory: Inverse method and prospective error analysis, *J. Geophys. Res.*, 113 doi: 10.1029/2006JD008336, 2008.
- Crisp D., Miller C. E., DeCola P. L.: NASA Orbiting Carbon Observatory: measuring the column averaged carbon dioxide mole fraction from space. *J. Appl. Remote Sens.*, 2, 023508, doi:10.1117/1.2898457, 2008.
- Crisp D. for the OCO-2 Team: Measuring Atmospheric Carbon Dioxide from Space with the Orbiting Carbon Observatory-2 (OCO-2), *Proc. SPIE 9607, Earth Observing Systems XX*, 960702, doi: 10.1117/12.2187291, 2015.
- Deutscher, N. M., Griffith, D. W. T., Bryant, G. W., Wennberg, P. O., Toon, G. C., Washenfelder, R. A., Keppel-Aleks, G., Wunch, D., Yavin, Y., Allen N. T., Blavier, J.-F., Jiménez R., Daube, B. C., Bright, A. V., Matross, D. M., Wofsy, S. C., and Park, S.: Total column CO₂ measurements at Darwin, Australia-site description and calibration against in situ aircraft profiles, *Atmos. Meas. Tech.*, 3, 947-958, doi:10.5194/amt-3-947-2010, 2010.
- Frankenberg, C., Pollock, R., Lee, R. A. M., Rosenberg, R., Blavier, J.-F., Crisp, D., O'Dell C. W., Osterman, G. B., Roehl, C., Wennberg, P. O., and Wunch, D.: The Orbiting Carbon Observatory (OCO-2): spectrometer performance evaluation using pre-launch direct sun measurements. *Atmospheric Measurement Techniques*, 8(1), 301–313. doi:10.5194/amt-8-301-2015, 2015.
- Hase, F., Blumenstock, T., and Paton-Walsh, C.: Analysis of the instrumental line shape of high resolution Fourier transform IR spectrometers with gas cell measurements and new retrieval software, *Appl. Optics*, 38, 3417–3422, doi:10.1364/AO.38.003417,1999.
- Hase, F., Drouin, B. J., Roehl, C. M., Toon, G. C., Wennberg, P. O., Wunch, D., Blumenstock, T., Desmet F., Feist, D. G., Heikkinen, P., De Mazière, M., Rettinger, M., Robinson, J., Schneider, M., Sherlock, V., Sussmann, R., Té Y., Warneke, T., and Weinzierl, C.: Calibration of sealed HCl cells used for TCCON instrumental line shape monitoring, *Atmospheric Measurement Techniques*, 6(12), 3527–3537, doi:10.5194/amt-6-3527-2013, 2013.

- Kiel, M., Wunch, D., Wennberg, P. O., Toon, G. C., Hase, F., and Blumenstock, T.: Improved retrieval of gas abundances from near-infrared solar FTIR spectra measured at the Karlsruhe TCCON station, *Atmos. Meas. Tech.*, 9(2), 669–682, doi:10.5194/amt-9-669-2016, 2016.
- 420 Kivi, R. and Heikkinen, P.: Fourier transform spectrometer measurements of column CO₂ at Sodankylä, Finland, *Geosci. Instrum. Method. Data Syst.*, 5, 271–279, 2016.
- Messerschmidt, J., Macatangay, R., Notholt, J., Petri C., Warneke, T., and Weinzierl, C.: Side by side measurements of CO₂ by ground-based Fourier transform spectrometry (FTS), *Tellus B*, 62(5), 749–758, doi:10.1111/j.1600-0889.2010.00491.x., 2010.
- 425 Messerschmidt, J., H. Chen, N. M. Deutscher, C. Gerbig, P. Grupe, K. Katrynski, F.-T. Koch, J. V. Lavrič, J. Notholt, C. Rödenbeck, W. Ruhe, T. Warneke, and Weinzierl, C.: Automated ground-based remote sensing measurements of greenhouse gases at the Białystok site in comparison with collocated in situ measurements and model data, *Atmospheric Chemistry and Physics*, 12(15), 6741–6755, doi:10.5194/acp-12-6741-2012, 2012.
- 430 Miao, R., Lu N., Yao L., Zhu, Y., Wang, J., and Sun, J.: Multi-Year Comparison of Carbon Dioxide from Satellite Data with Ground-Based FTS Measurements (2003–2011), *Remote Sensing*, 5(7), 3431–3456, doi:10.3390/rs5073431, 2013.
- Miller, C. E., Crisp, D. DeCola, P. L., Olsen, S. C., Randerson, J. T., Michalak, A. M., Alkhaled, A., Rayner, P., Jacob, D. J., Suntharalingam, P., Jones, D. B. A., Denning, A. S., Nicholls, M. E., Doney, 435 S. C., Pawson, S., Boesch, H., Connor B. J., Fung I. Y., O'Brien, D., Salawitch, R. J., Sander, S. P., Sen, B., Tans, P., Toon, G. C., Wennberg, P. O., Wofsy, S. C., Yung, Y. L., and Law, R. M.: Precision requirements for space-based XCO₂ data, *J. Geophys. Res-Atmos.*, 109, D02301, doi: 10.1029/2006JD007659, 2007.
- Morino, I., Uchino, O., Inoue, M., Yoshida, Y., Yokota T., Wennberg, P. O., Toon, G. C., Wunch, D., 440 Roehl, C. M., Notholt, J., Warneke, T., Messerschmidt, J., Griffith, D. W. T., Deutscher, N. M., Sherlock, V., Connor, B. J., Robinson, J., Sussmann, R., and Rettinger, M.: Preliminary validation of column-averaged volume mixing ratios of carbon dioxide and methane retrieved from GOSAT short-wavelength infrared spectra, *Atmospheric Measurement Techniques*, 4(6), 1061–1076, doi:10.5194/amt-4-1061-2011, 2011.
- 445 O'Dell, C. W., Connor, B., Bösch, H., O'Brien, D., Frankenberg C., Castano, R., Christi, M., Eldering, D., Fisher, B., Gunson, M., McDuffie, J., Miller, C. E., Natraj, V., Oyafuso, F., Polonsky, I., Smyth, M., Taylor, T., Toon, G. C., Wennberg, P. O., and Wunch, D.: The ACOS CO₂ retrieval algorithm – Part 1: Description and validation against synthetic observations, *Atmospheric Measurement Techniques*, 5, 99–121, doi: 10.5194/amt-5-99-2012, <http://www.atmos-meas-tech.net/5/99/2012/>, 450 2012.
- Ohyama, H., Morino, I., Nagahama, T., Machida, T., Suto H., Oguma, H., Sawa, Y., Matsueda, H., Sugimoto, N., Nakane, H., and Nakagawa, K.: Column-averaged volume mixing ratio of CO₂

- measured with ground-based Fourier transform spectrometer at Tsukuba, *J. Geophys. Res.*, 114, D18303 doi:10.1029/2008JD011465, 2009.
- 455 Ohyama, H., Kawakami, S., Tanaka, T., Morino, Uchino, I., O., Inoue, M., Sakai, T., Nagai, T., Yamazaki, A., Uchiyama, A., Fukamachi, T., Sakashita, M., Kawasaki, T., Akaho, T., Arai, K., and Okumura, H.: Observations of XCO₂ and XCH₄ with ground-based high-resolution FTS at Saga, Japan, and comparisons with GOSAT products, *Atmos. Meas. Tech.*, 8(12), 5263–5276, doi:10.5194/amt-8-5263-2015.
- 460 Rayner P. J., and O'Brien D. M.: The utility of remotely sensed CO₂ concentration data in surface source inversions, *Geophys. Res. Lett.*, 28, 175–178, doi: 10.1029/2000GL011912, 2001.
- Schneising O., Buchwitz M., Burrows J. P., Bovensmann, H., Reuter, M., Notholt, J., Macatangay, R., and Warneke, T.: Three years of greenhouse gas column-averaged dry air mole fractions retrieved from satellite-Part 1: Carbon dioxide, *Atmos. Chem. Phys.*, 8, 3827-3853, 2008.
- 465 Sun, Y., Palm, M., Weinzierl, C., Peteri, C., Notholt, J., Wang, Y., and Liu, C.: Technical note: Sensitivity of instrumental line shape monitoring for the ground-based high-resolution FTIR spectrometer with respect to different optical attenuators, *Atmos. Meas. Tech. Discuss.*, doi:10.5194/amt-10-989-2017.
- Thoning, K. W., Tans, P. P. and Komhyr, W. D.: Atmospheric carbon dioxide at Mauna Loa
470 Observatory. Analysis of the NOAA GMCC Data, 1974-1985, *J. Geophys. Res.*, 94, 8549-8565, 1989.
- WMO (2016). The state of greenhouse gases in the atmosphere based on global observations through 2015, greenhouse gas. *Greenhouse Gas Bulletin 2016*. https://library.wmo.int/opac/doc_num.php.
- Wang, W., Tian, Y., Liu, C., Sun, Y., Liu, W., Xie, P., Liu, J., Xu, J., Morino, I., Velazco, V., Griffith,
475 D., Notholt, J., and Warneke, T.: Investigating the performance of a greenhouse gas observatory in Hefei, China, *Atmos. Meas. Tech.*, 10, 2627–2643, 2017.
- Wang, Y., Munger, J. W., Xu, S., McElroy, M. B., Hao, J., Nielsen, C. P., and Ma, H.: CO₂ and its correlation with CO at a rural site near Beijing: implications for combustion efficiency in China, *Atmos. Chem. Phys.*, 10, 8881–8897, <https://doi.org/10.5194/acp-10-8881-2010>, 2010.
- 480 Washenfelder R. A., Toon G. C., Blavier J-F., Yang Z., Allen N. T., Wennberg P. O., Vay S. A., Matross, D. M., and Daube B. C.: Carbon dioxide column abundances at the Wisconsin Tall Tower site, *Journal of Geophysical Research*, 2006, 111, doi:10.1029/2006JD00715, 2006.
- Warneke, T., Yang, Z., Olsen, S., Korner, S., Notholt J., Toon, G. C., Velazco, V., Schultz, A., and Schrems, O.: Seasonal and latitudinal variations of column averaged volume-mixing ratios of
485 atmospheric CO₂, *Geophysical Research Letters*, 32(3), 2-5, doi:10.1029/2004GL021597, 2005.
- Wunch, D., Toon G. C., Wennberg, P. O., Wofsy, S. C., Stephens, B., Fisher, M. L., Uchino O., Abshire, J. B., Bernath, P. F., Biraud, S. C., Blavier, J.-F. L., Boone, C. D., Bowman, K. P., Browell, E. V., Campos, T., Connor, B. J., Daube, B. C., Deutscher, N. M., Diao M., Elkins, J. W., Gerbig, C.,

490 Gottlieb, E., Griffith, D. W. T., Hurst, D. F., Jiménez, R., Keppel-Aleks, G., Kort, E. A., Macatangay,
R., Machida, T., Matsueda, H., Moore, F. L., Morino, I., Park, S., Robinson, J., Roehl, C. M., Sawa,
Y., Sherlock, V., Sweeney, C., Tanaka, T., and Zondlo, M. A.: Calibration of the Total Carbon
Column Observing Network using aircraft profile data, *Atmospheric Measurement Techniques*, 3(5),
1351-1362, doi:10.5194/amt-3-1351-2010.

495 Wunch, D., Toon, G. C., Sherlock, V., Deutscher, N. M., Liu X., Feist, D. G., and Wennberg, P. O.:
The Total Carbon Column Observing Network's GGG2014 Data Version.
doi:10.14291/tccon.ggg2014.documentation.R0/1221662, 2015.

Wunch, D., Wennberg, P.O., Osterman, G., Fisher, B., Naylor, B., Roehl, C. M., O'Dell, C., Mandrake,
L., Viatte, C., Griffith, D. W. T., Deutscher, N. M., Velazco, V. A., Notholt, J., Warneke, T., Petri, C.,
Maziere, M. De, Sha, M. K., Sussmann, R., Rettinger, M., Pollard, D., Robinson, J., Morino, I.,
500 Uchino O., Hase, F., Blumenstock, T., Kiel, M., Feist, D. G., Arnold S.G., Strong, K., Mendonca, J.,
Kivi, R., Heikkinen, P., Iraci, L., Podolske, J., Hillyard, P. W., Kawakami, S., Dubey, M. K., Parker,
H. A., Sepulveda, E., Rodriguez, O. E. G., Te, Y., Jeseck, P., Gunson, M. R., Crisp, D., and Eldering
A., Comparisons of the Orbiting Carbon Observatory-2 (OCO-2) XCO₂ measurements with TCCON,
Atmos. Meas. Tech. Discuss., doi:10.5194/amt-2016-227, 2016.

505

510

515

520

Table.1 Measurement setting for the Anmyeondo g-b FTS spectrometer of the Bruker 125HR model.

Item	Setting
Aperture	0.8 mm
Detectors	RT-Si Diode DC, RT-InGaAs DC
Beamsplitters	CaF ₂
Scanner velocity	10 kHz
Low pass filter	10 kHz
High folding limit	15798.007031
Spectral Resolution	0.02 cm ⁻¹
Optical path difference	45 cm
Acquisition mode	Single sided, forward backward
Sample scan	2 scans
Sample scan time	~110 s

Table. 2 Spectral windows used for the retrievals of the columns of CO₂ and O₂.

Gas	Center of spectral window (cm ⁻¹)	Width (cm ⁻¹)	Interfering gas
O ₂	7885.0	240.0	H ₂ O, HF, CO ₂
CO ₂	6220.0	80.0	H ₂ O ,HDO, CH ₄
CO ₂	6339.5	85.0	H ₂ O ,HDO

535 **Table. 3** The statistical results for XCO₂ and XCH₄ comparisons between aircraft and g-b FTS are summarized.

Instruments (Aircraft vs. g-b FTS)	No. of coincident measurement	Absolute difference (ppm)	Relative diff. (%)
XCO ₂	3	-0.798 ± 1.734	-0.196 ± 0.427
XCH ₄	3	-0.0079 ± 0.012	-0.426 ± 0.632

Table. 4 Annual mean of XCO₂, XCO, and XCH₄ from Anmyeondo g-b FTS from 2014 to 2016 is given.

Gases	Annual mean ± standard deviation		
	2014	2015	2016
XCO ₂ (ppm)	396.91 ± 2.55	399.32 ± 2.96	402.97 ± 2.74
XCO (ppb)	99.42 ± 14.71	102.73 ± 14.91	105.39 ± 10.68
XCH ₄ (ppm)	1.837 ± 0.014	1.844 ± 0.015	1.864 ± 0.015

540

Table. 5 Summary of the statistics of XCO₂ comparisons between OCO-2 and the g-b FTS from 2014 to 2016 are presented. N - coincident number of data, R - Pearson correlation coefficient, RMS - Root Mean Squares differences.

545

N	Mean Absolute. diff. (ppm)	Mean Relative diff (%)	R	RMS (ppm)
13	0.18±1.19	0.04±0.29	0.94	1.16

Table. 6 Seasonal mean and standard deviations of XCO₂ from the g-b FTS and OCO-2 in the period between 2014 and 2016 are given below.

550

Season	g-b FTS XCO ₂ mean ± std (ppm)	OCO-2 XCO ₂ mean ± std (ppm)
Winter	401.52 ± 0.85	402.67 ± 2.67
Spring	402.72 ± 2.79	403.96 ± 2.77
Summer	396.92 ± 3.28	399.68 ± 3.77
Autumn	398.01 ± 2.83	398.48 ± 2.41

555

Figures

560

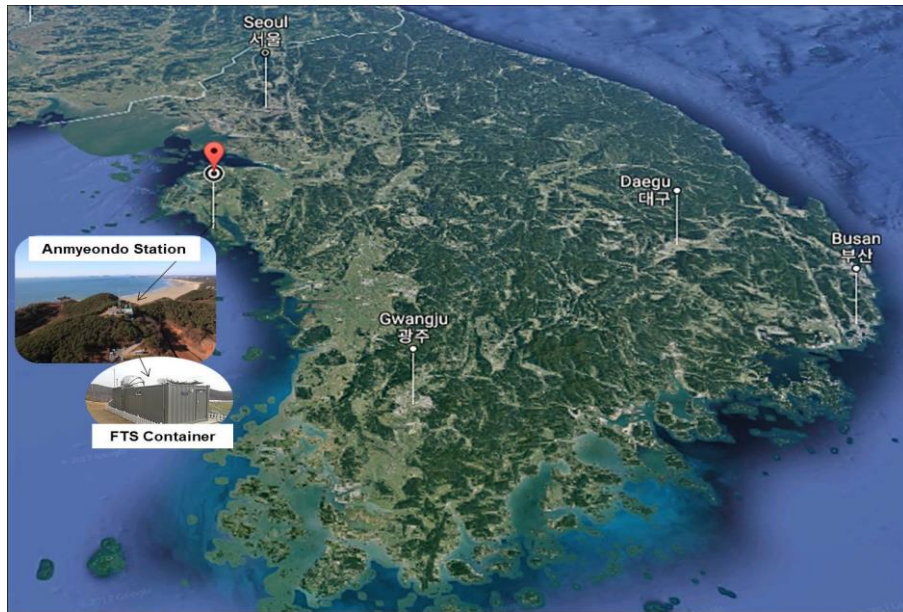


Figure 1. Anmyeondo (AMY) g-b FTS station.

565

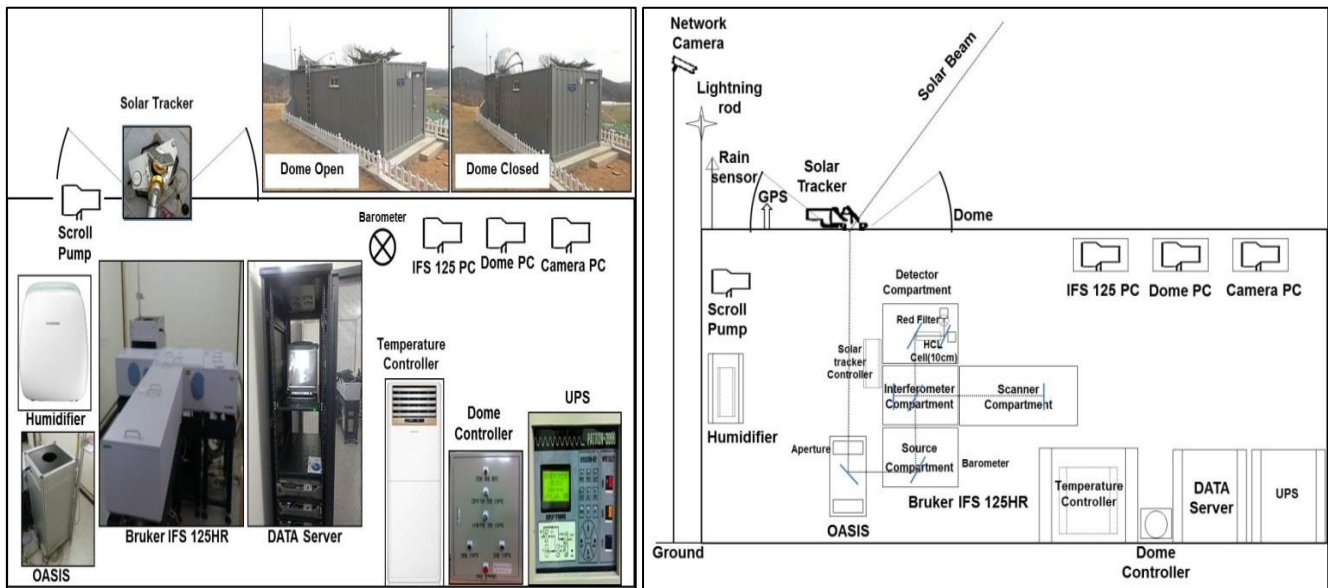


Figure 2. Photographs of the automated FTS laboratory. The Bruker Solar Tracker type A547 is mounted in the custom made dome. A servo controlled solar tracker directs the solar beam through a CaF_2 window to the FTS (125HR) in the laboratory. The server computer is used for data acquisition. PC1 and PC2 are used for controlling the spectrometer, solar tracker, dome, camera, pump, GPS satellite time, and humidity sensor.

575

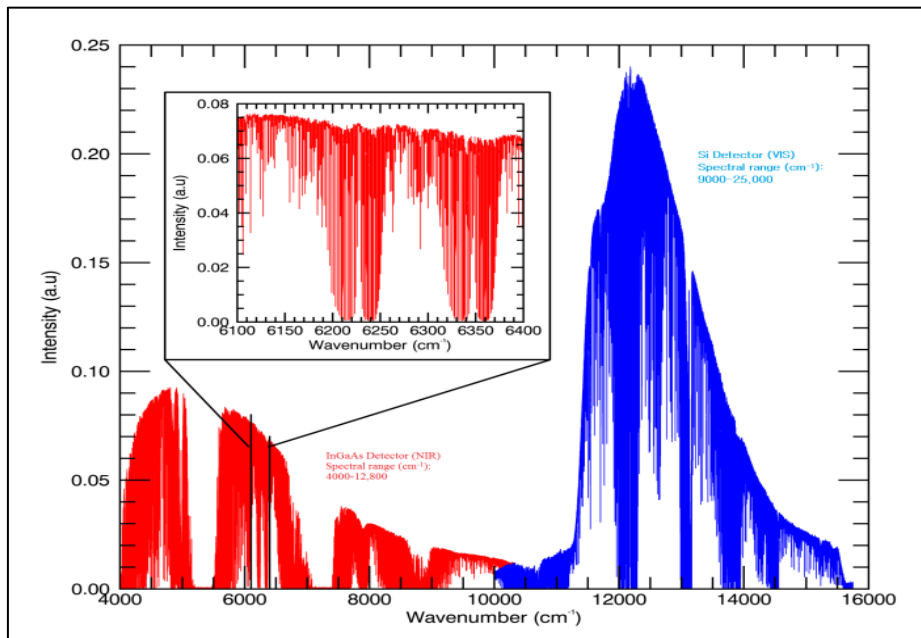


Figure 3. Single spectrum recorded on 4 October 2014 with a resolution of 0.02 cm^{-1} . A typical example for the spectrum of XCO_2 is shown in the inset.

580

585

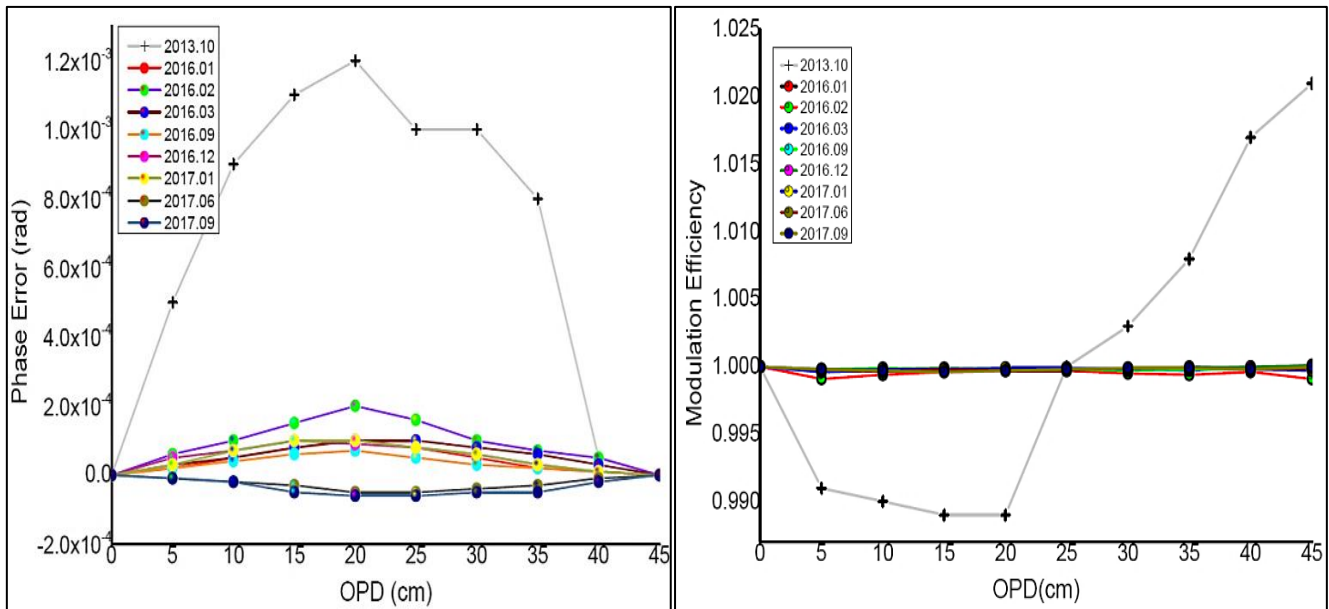


Figure 4. Phase error (rad) (left panel) and Modulation efficiency (right panel) of HCl measurements from the g-b FTS are displayed in the period from October 2013 to September 2017. Resolution = 0.015 cm^{-1} , Aperture = 0.8 mm.

590

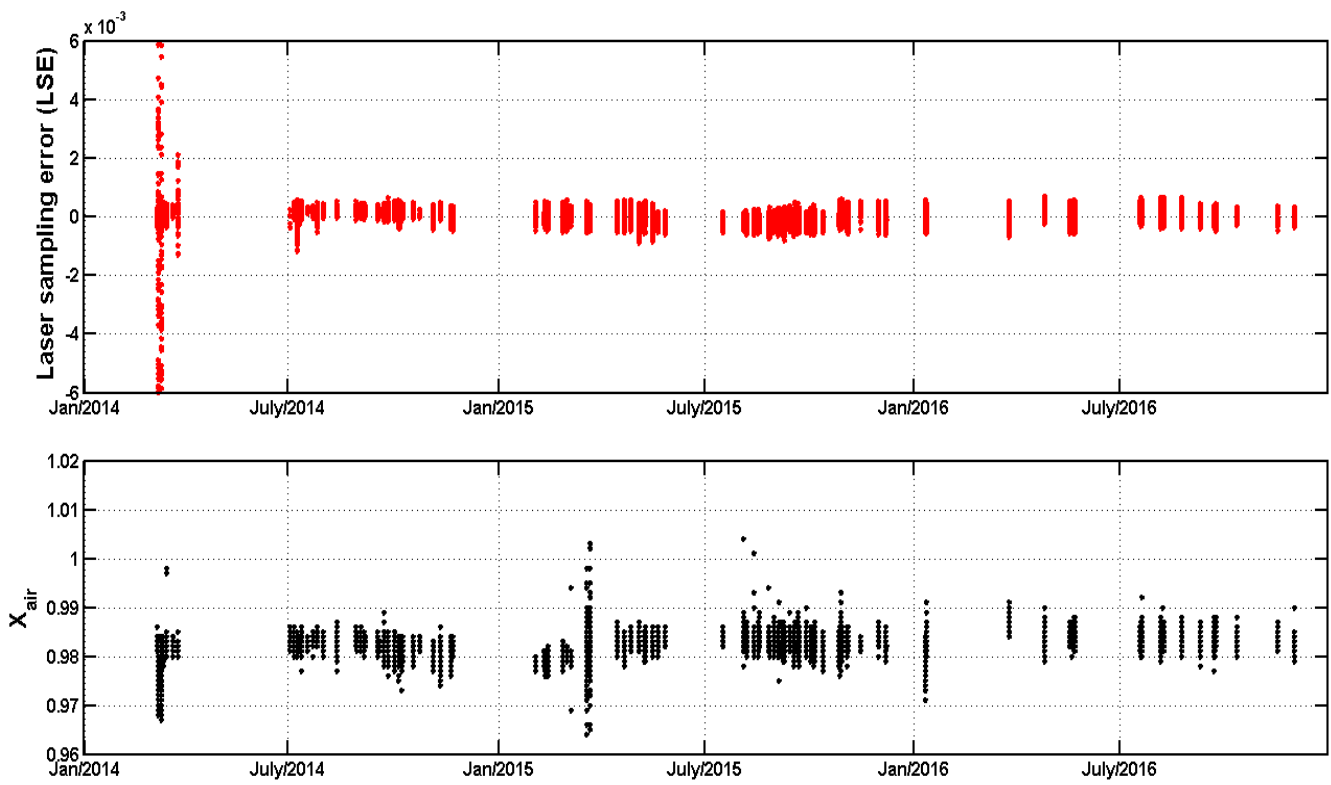


Figure 5. Time series of LSE (top panel) and X_{air} (bottom panel) from the g-b FTS during 2014- 2016 is shown. Each marker represents a single measurement.

595

600

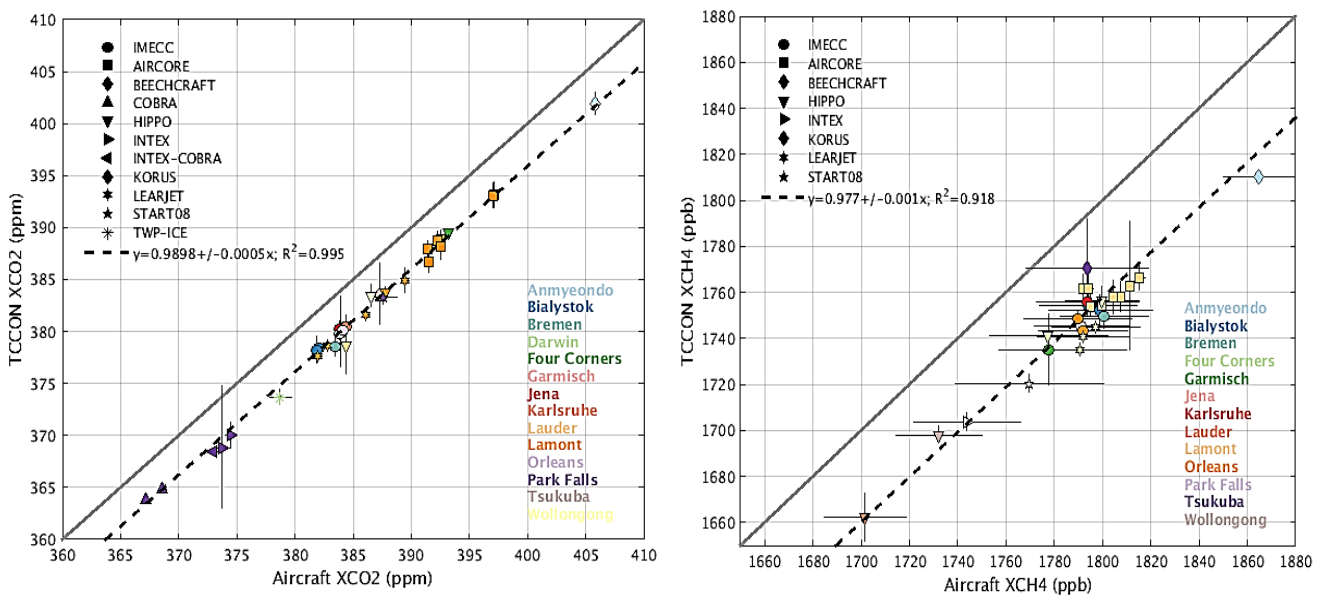


Figure 6. The comparisons of X_{CO_2} and X_{CH_4} between the aircraft observation and TCCON sites data are shown. The left side is X_{CO_2} and the right side is X_{CH_4} (light blue depicts for Anmyeondo station).

605

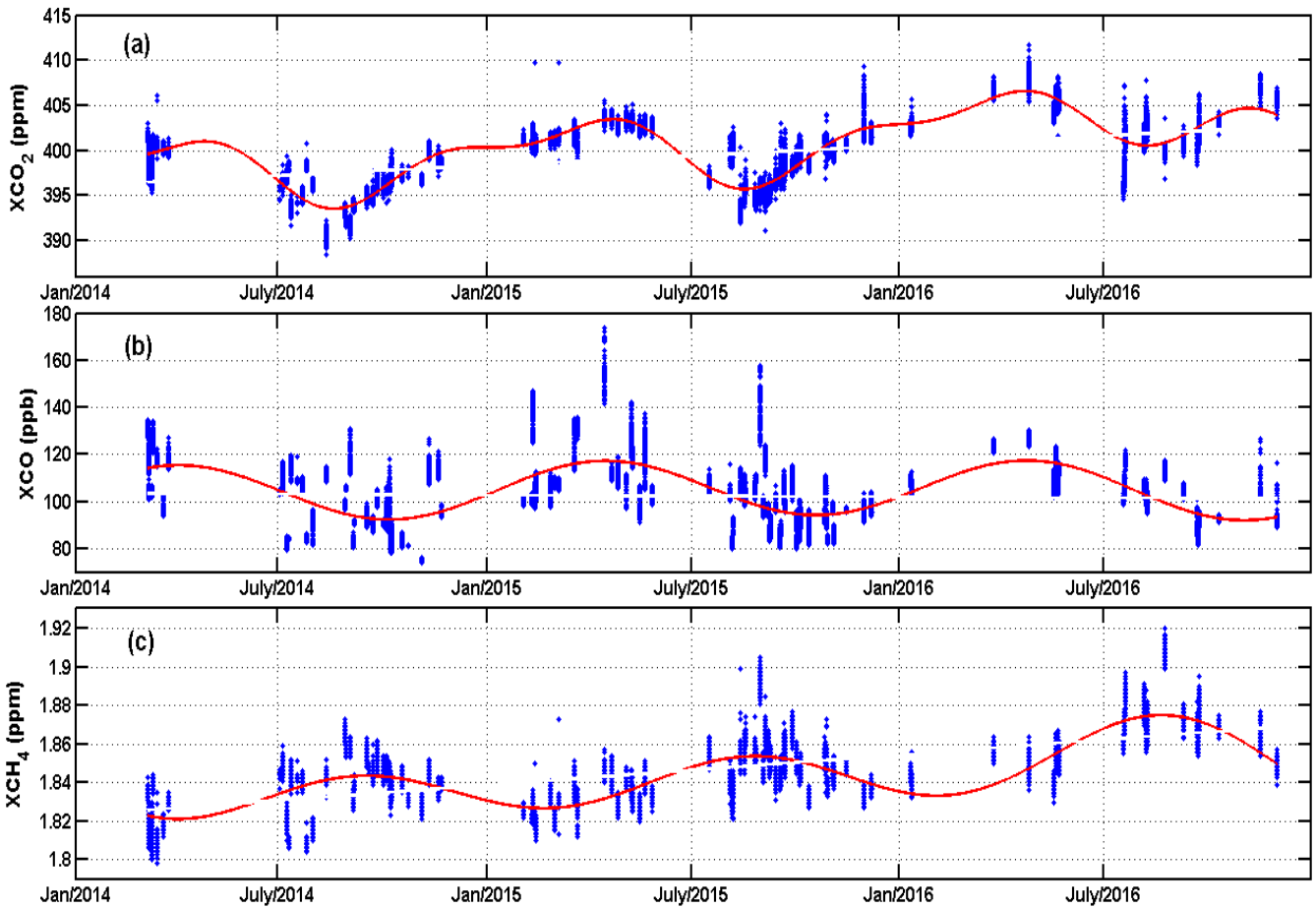
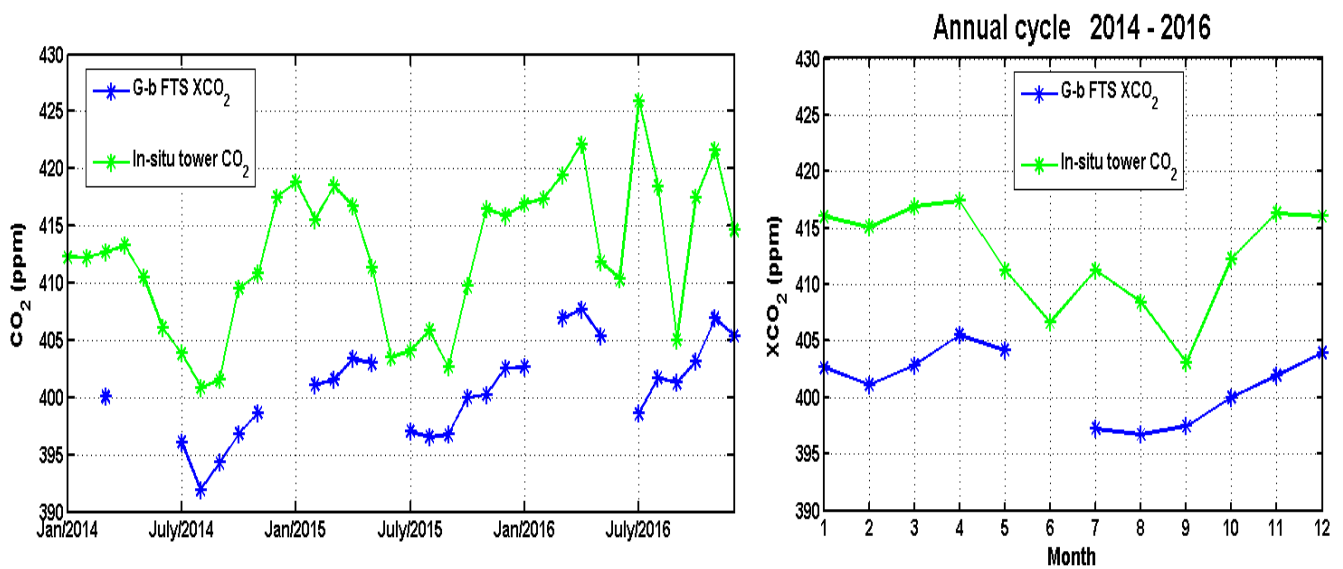


Figure 7. Time series of XCO_2 , XCO , and XCH_4 from top to bottom panels (a-c), respectively in the period between February 2014 and December 2016 is given. Each marker indicates a single retrieval. Fitting curves (red solid lines) are also displayed.

610



615 **Figure 8.** Left panel shows the time series of FTS XCO_2 and in-situ tower CO_2 on monthly mean basis, whereas right panel depicts annual cycle.

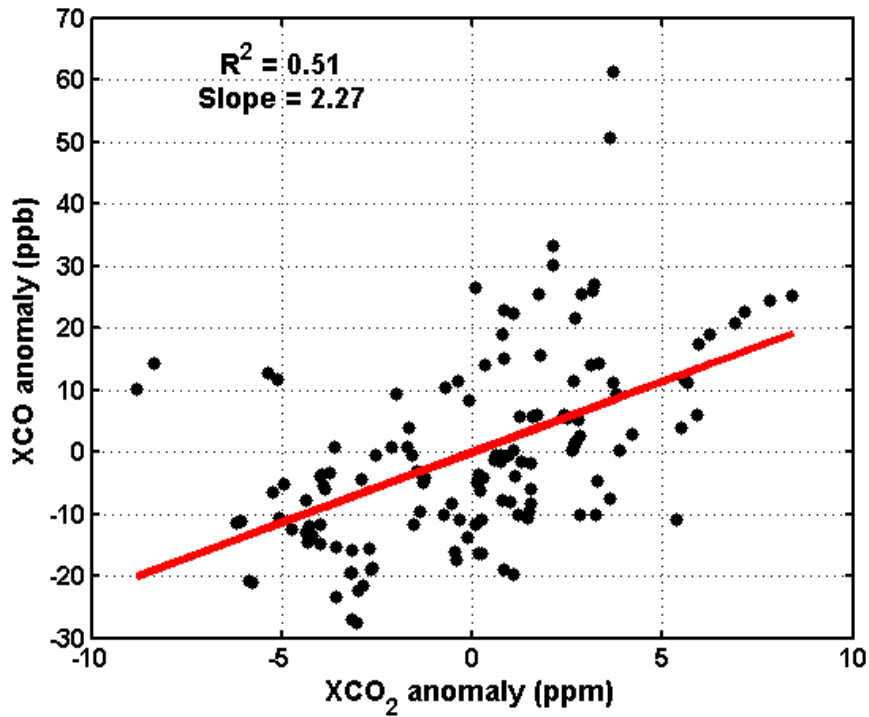


Figure 9. Correlation between XCO₂ versus XCO anomalies at Anmyeondo FTS station between February 2014 and December 2016, excluding summer data, is depicted.

620

625

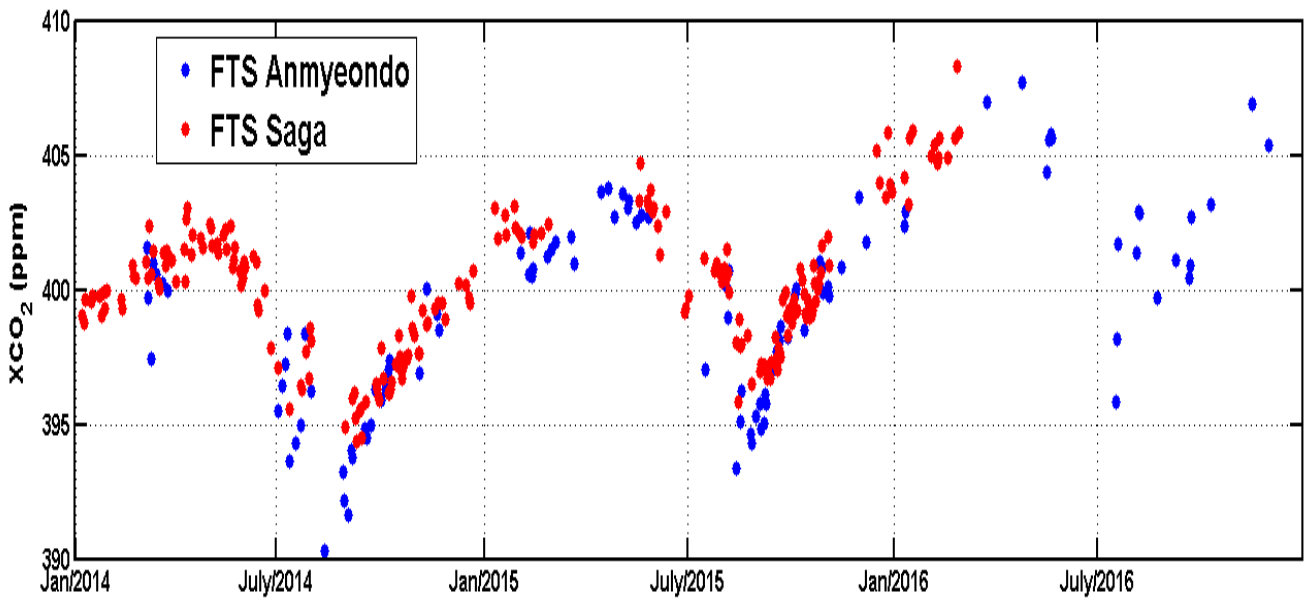


Figure 10. Time series of XCO₂ retrieval from Anmyeondo FTS and Saga FTS in the period of February 2014 to December 2016 is depicted.

630

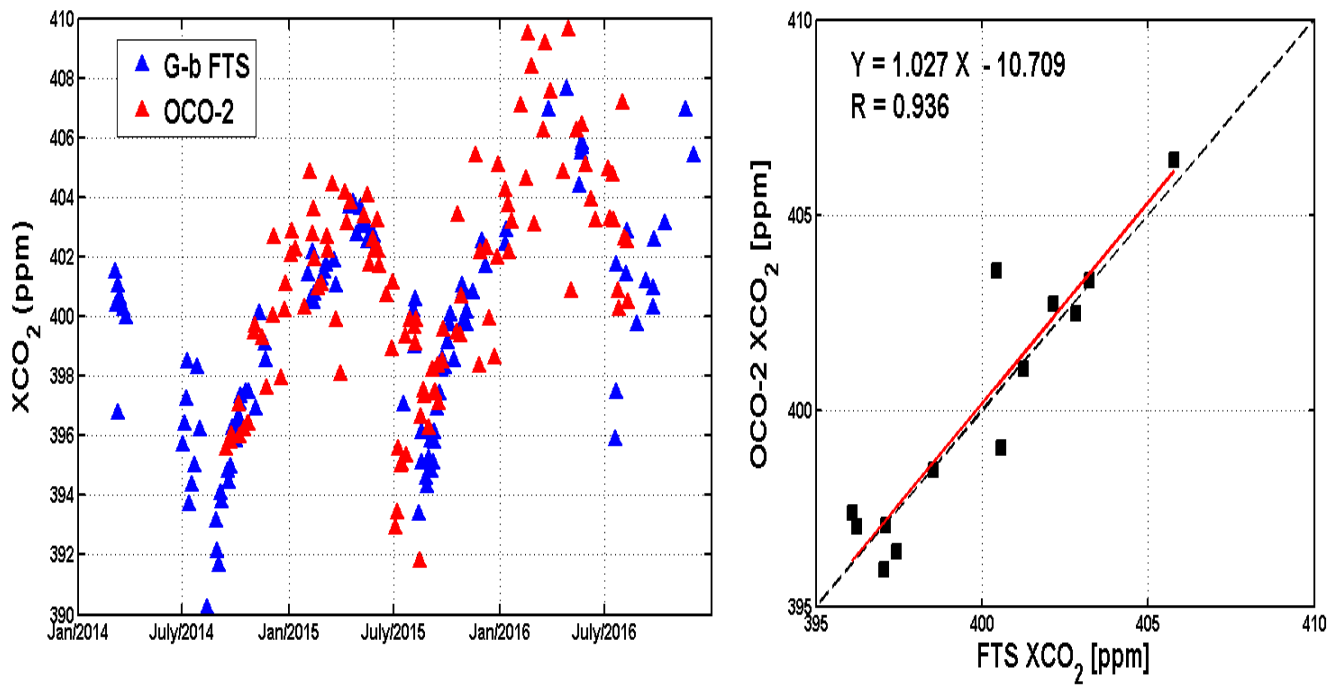


Figure 11. Left panel: The time series of XCO₂ from the g-b FTS (blue triangle) and OCO-2 (red triangle) over the Anmyeondo station from February 2014 to December 2016 are shown. Right panel: The linear regression curve between FTS and OCO-2 is shown. All results are given on daily medians basis.

635